On Modelling of the Hole Erosion Test

Stéphane Bonelli, Nadia Benahmed, Olivier Brivois

ICSE, 3rd International Conference on Scour and Erosion
1-3 nov 2006, Amsterdam

On Modelling of the Hole Erosion Test

S.Bonelli*, N. Benahmed* and O. Brivois*,**
* Cemagref/Hydraulics Engineering and Hydrology Research Unit, Aix-en-Provence, France
** CNRS/Mechanics and Acoustics Laboratory, Marseille, France

I. Introduction

Internal erosion of soil resulting from seepage flow is the main cause of serious hydraulic work (dykes, dams) failure, in terms of the risk of flooding areas located downstream. When internal erosion is suspected of occurring or has already been detected in situ, the time to failure is difficult to predict. To be able to develop effective emergency action plans preventing heavy casualties and damage to property, it is necessary to have a characteristic time to use as a basis.

During the last few decades, several laboratory studies have been carried out on internal erosion. Four types of internal erosion process have been identified in particular: 1) evolution of defects (cracks and microfissures) in the soil matrix, 2) regressive erosion, 3) internal suffusion, which affects the soil structure, 4) external suffusion between two soils. The present study concerns the first process: the enlargement of a crack, which leads to an internal erosion process known as "piping" in soil mechanics.

Several experimental methods have been developed for simulating the internal erosion process experimentally, and various types of equipment have been developed for performing hole erosion tests [3], [12], [13]. However, few attempts have been made to model these tests. The aim of this study was to draw up a useful model for interpreting hole erosion tests.

In the first part of this paper, equations for diphasic flow and equations of jump with erosion are presented. In the second part, a model is developed by spatially integrating simplified equations obtained from asymptotic developments in the case of a circular hole. Some comparisons are made in the third part between the model and experimental data.

II. Two-phase flow equation with interface erosion

It is proposed to study the surface erosion of a fluid/soil interface subjected to a flow running parallel to the interface. The soil, which is taken here to be saturated, is eroded by the flow, which then carries away the eroded particles. As long as the particles are small enough in comparison with the characteristic length scale of the flow, this two-phase flow can be said to be a continuum. We take Ω to denote the volume of the two-phase mixture and Γ the fluid/soil interface. For the sake of simplification, sedimentation and deposition processes are neglected. The mass conservation equations for the water/particles mixture and for the mass of the particles as well as the balance equation of momentum of the mixture within Ω can be written as follows in a Eulerian framework [6], [10]:

$$\frac{\partial \rho}{\partial t} + \vec{\nabla} \cdot (\rho \vec{u}) = 0 \,, \tag{1}$$

$$\frac{\partial \rho Y}{\partial t} + \vec{\nabla} \cdot (\rho Y \vec{u}) = -\vec{\nabla} \cdot \vec{J} \,, \tag{2}$$

$$\frac{\partial \rho \vec{u}}{\partial t} + \vec{\nabla} \cdot (\rho \vec{u} \otimes \vec{u}) = \vec{\nabla} \cdot \boldsymbol{\sigma} \,. \tag{3}$$

In these equations, ρ is the density of the mixture, depending on the particles mass fraction Y, $\vec{u}$ is the mass-weighted average velocity, $\vec{J}$ is the mass diffusion of the flux of particles, and $\boldsymbol{\sigma}$ is the Cauchy stress tensor in the mixture.

The two media (i.e. the soil and the two-phase fluid) are separated by the interface Γ. The water/particle mixture is assumed to flow like a fluid above Γ, while a solid-like behaviour is taken to occur below Γ. As there is a process of erosion, a mass flux crosses this interface and undergoes a transition from solid-like to fluid-like behaviour. Γ is therefore not a material interface: at different moments, Γ is not defined by the same particles. We assume Γ to be a purely geometric separating line which has no thickness. Let us take $\vec{n}$ to denote the normal unit vector of Γ oriented outwards from the soil, and $\vec{v}_\Gamma$ to denote the normal velocity of Γ. The jump equations over Γ are [9]

$$\left[\!\left[\rho(\vec{v}_\Gamma - \vec{u}) \cdot \vec{n} \right]\!\right] = 0 \,, \tag{4}$$

$$\left[\!\left[\rho Y(\vec{v}_\Gamma - \vec{u}) \cdot \vec{n} \right]\!\right] = \left[\!\left[\vec{J} \cdot \vec{n} \right]\!\right], \tag{5}$$

$$\left[\!\left[\rho \vec{u}(\vec{v}_\Gamma - \vec{u}) \cdot \vec{n} \right]\!\right] = -\left[\!\left[\boldsymbol{\sigma} \cdot \vec{n} \right]\!\right], \tag{6}$$

This project was sponsored by the Région Provence Alpes Côte d'Azur. This research project is continuing under the sponsorship of the French National Research Agency under grant 0594C0115 (ERINOH).

where $[\![a]\!] = a_g - a_b$ is the jump of any physical variable a across the interface, and a_g and a_b stands for the limiting value of a on the solid and fluid sides of the interface, respectively. The soil is assumed to be homogeneous, rigid and devoid of seepage. The co-ordinate system depends on the soil in question. The total flux of eroded material (both particles and water) crossing the interface is therefore $\dot{m} = -\rho_g \vec{v}_\Gamma \cdot \vec{n}$, where ρ_g is the density of the soil.

Erosion laws dealing with soil surface erosion by a tangential flow are often written in the form of threshold laws such as [2]:

$$\dot{m} = \begin{cases} k_{er}(\left|\tau_b\right| - \tau_c) \text{ if } \left|\tau_b\right| > \tau_c \\ 0 \text{ otherwise} \end{cases}, \qquad (7)$$

with

$$\left|\tau_b\right| = \sqrt{(\boldsymbol{\sigma}\cdot\vec{n})^2 - (\vec{n}\cdot\boldsymbol{\sigma}\cdot\vec{n})^2}\Big|_b . \qquad (8)$$

where τ_c is the critical (threshold) shear stress involved in the erosion, k_{er} is the coefficient of soil erosion, and $\left|\tau_b\right|$ is the tangential shear stress at the interface.

This complete set of equations was previously used to study various situations involving a permanent flow (boundary layer and free surface flow) over an erodable soil [1]. The use of these equations is extended here to the study of internal erosion by introducing a spatial integration over Ω.

III. APPLICATION TO PIPING EROSION

Let us take a cylinder Ω with length L and radius R (initial value R_0) (Fig. 1). Reference velocity is $V_{fl} = Q_{fl} / \pi R_0^2$, where Q_{fl} is the initial input flow and the flow time is $t_{fl} = R_0 / V_{fl}$. By assuming that this is axisymmetrical flow, we eliminated one momentum equation. We introduced the small parameter R_e^{-1} to simplify the dimensionless equations in a boundary layer theory spirit ([8],[11]), where the Reynolds number $R_e = V_{fl} R_0 / \nu_f$ was assumed to be large and ν_f is the kinematic viscosity. Navier-Stokes equations were written with the time scaled by t_{fl}, the axial coordinate by $R_0 R_e$, the radial coordinate by R_0, the axial velocity by V_{fl}, the radial velocity by V_{fl} / R_e, and the stresses by $\rho_f V_{fl}^2$. Assuming turbulent stress viscosity and diffusivity, we performed the regular asymptotic expansion of the unknowns and we neglected the terms of order $\mathrm{O}(R_e^{-1})$ in (1) and (2) (as in [1]). We therefore now had a single momentum equation, and the pressure was uniform across any section.

We integrated the system obtained first on a cross section, and secondly along the axis. We take $< a >_R$ to denote the mean value of a in a cross section, and $< a >_\Omega$ to denote the mean value in Ω. The mean longitudinal velocity is $V =< u >_R$. The mean density of the fluid is $\overline{\rho} =< \rho >_\Omega$. The following assumptions were made : A1) the tangential velocities were taken to be continuous across Γ (no-slip condition at the interface), A2) the radial profile of the velocity field was given by the Nikuradze approximation, A3) the concentration was uniform over a given section and linear along the axis, A4) we introduced a phenomenological friction coefficient f_b by $\tau_b = f_b \overline{\rho} V^2$, A5) the radius R was axially uniform (and therefore , $V =< u >_\Omega$). This gave an ordinary differential system with unknowns $(R, \overline{\rho}, V)$ which can be solved numerically.

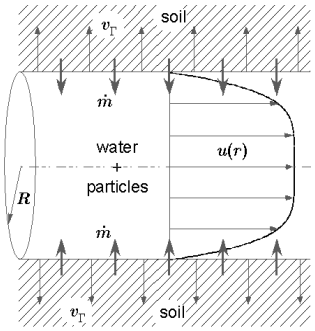

Figure 1. Sketch of the axisymmetrical flow process involving erosion of the soil and transport of the eroded particles.

If the erosion time scale is suitably chosen, dimensional analysis shows that the four basic parameters of the system are:

$$\tilde{a}_\phi = \frac{R_0 \rho_g}{f_b L \rho^f}, \; \tilde{b}_\phi = \left(\frac{< u^2 >_\Omega}{< u >_\Omega^2} - 1\right)\left(1 - \frac{\rho^f}{\rho_g}\right) \qquad (9)$$

$$\tilde{k}_{ref} = \frac{k_{er} V_{fl}}{1 + k_{er} V_{fl}}, \; \tilde{\tau}_c = \frac{\tau_c}{P_{fl}} \qquad (10)$$

The stress $P_{fl} = R_0(p_{in} - p_{out}) / 2L$ reflects the hydraulic gradient and depends on the input and output pressures, respectively p_{in} and p_{out}.

The erosion velocity turns out to be $V_{er} = k_{er} P_{fl} / (1 + k_{er} V_{fl}) \rho_g$. The eroded flow is thus $Q_{er} = 2\pi R_0 L V_{er}$ and the erosion time is $t_{er} = R_0 / V_{er}$. The erosion flow scale ratio is therefore $Q_{er} / Q_{fl} = \alpha \tilde{k}_{ref} \tilde{a}_\phi^{-1}$, the erosion time scale ratio is $t_{fl} / t_{er} = \tilde{k}_{ref} f_b \rho^f / \rho_g$. The maximum volumic concentration is $c_{ref} = (1 - n) / (1 + \tilde{a}_\phi \tilde{k}_{ref}^{-1})$, where n is the porosity of the soil.

We assumed that $\tilde{a}_\phi \geq \mathrm{O}(1)$ and $\tilde{b}_\phi \approx \mathrm{O}(1)$, which is the case in the experiments described below. We call $\tilde{k}_{ref}$ the kinetics of erosion (dimensionless) number. If

$\tilde{k}_{ref} \ll 1$ is a small parameter, then asymptotic analysis will yield important conclusions: 1) the concentration will be low and becomes a secondary unknown, as it does not influence the density, the inertia, the velocity or the stress, 2) the flow will be quasi steady, 3) the interface velocity will be low and will not contribute to the inertia. We call this case, which arises when $k_{er} \ll V_{fl}^{-1}$, the low kinetics of erosion situation.

Starting with the initial condition $(R(0) = R_0, V(0) = 0)$, under the constant hydraulic gradient $P_{fl} > \tau_c$, the solution of the system can be written as follows:

$$\frac{R(t)}{R_0} = 1 + \left(1 - \frac{\tau_c}{P_{fl}}\right)\left[\exp\left(\frac{t}{t_{er}}\right) - 1\right], \quad (10)$$

$$\frac{V(t)}{V_{fl}} = \sqrt{\frac{R(t)}{R_0}}\ , \quad (11)$$

$$t_{er} = \frac{2L\rho_g}{k_{er}(p_{in} - p_{out})}. \quad (12)$$

The shear stress at the interface and the flow are given by:

$$\frac{\tau_b(t)}{P_{fl}} = \frac{R(t)}{R_0}, \frac{Q(t)}{Q_{fl}} = \left(\frac{R(t)}{R_0}\right)^{5/2}. \quad (13)$$

It should be noted that the limiting case $\tilde{k}_{ref} \to 1$ (corresponding to $k_{er} \to \infty$) can be of interest. In this case, the concentration can be high, and even reaching the soil compacity level $c_{ref} = (1-n)/(1+\tilde{a}_\phi)$. The erosion law (3) leads to $\tau_b = \tau_c$, but the rheological law depends stronglyon the concentration [7] (assumption A4 therefore has to be modified), and so the velocity remains unknown. Moreover, the concentration probably affects the velocity profile: assumptions A2 and A4 are no longer relevant. To our knowledge, radial profiles of concentrations in pipe flow with erosion have not yet been investigated.

IV. COMPARISON WITH EXPERIMENTAL DATA

According to the logic of the derivation given above, the scaling laws previously obtained (10) and (11) should hold in all past and future experiments performed on erosional pipe flow with a constant pressure drop involvinglow erosion kinetics. The folllowing comparisons with experimental data confirm the validity of this statement .

The Hole Erosion Test was designed to simulate piping flow erosion in a hole [3]. The soil specimen is compacted in a standard mould used for the Standard Compaction Test. A hole is drilled along the longitudinal axis of the soil sample. An eroding fluid is driven through the soil sample to initiate erosion of the soil along the pre-formed hole. The results of the test are given in terms of the flow rate versus time curve under a constant pressure drop. For further details about this test, see [3], [12], [13].

The predicted scaling law is now compared with previously published data [3]. Simulations were performed in 17 tests, using 10 different soils (clay, sandy clay, clayey sand or silty sand). Table I contains geological origin, particle size distribution and particle density of soils samples. Table II contains geotechnical properties of soil samples. Table III contains parameters of the hole erosion tests. Table IV contains results of the modelling of these tests with the scaling law (10) and (11). The initial radius and the length of the pipe were R_0=3 mm and L=117 mm. Since the $\tilde{a}_\phi$ numbers ranged from 2.37 to 4.82, and the $\tilde{k}_{er}$ numbers, from 7.54 10^{-5} to 1.19 10^{-2}, low erosion kinetics were present in all the cases studied.

Fig. 2 gives the increase in the flow in $Q \propto R^{5/2}$, and shows that the use of t_{er} leads to efficient dimensionless scaling. In Fig. 3, experimental data from [3] are plotted in the $(R(t)/R_0 - \tau_c/P_{fl},\ t/t_{er} + \ln(1-\tau_c/P_{fl}))$ plane. Nearly all the data can be seen to fall on a single curve. Thanks to the many simplifying assumptions, the agreement with the scaling law (4) speaks for itself: in spite of the large range of k_{er} (three orders of magnitude),

TABLE I.
GEOLOGICAL ORIGIN, PARTICLE SIZE DISTRIBUTION AND PARTICLE DENSITY OF SOIL SAMPLES

Soil	Geological Origin	%Gravel	%Sand	%Fines	%Finer than 0.002mm	Soil Particle Density
Bradys	Residual	1	24	75	48	2.74
Fattorini	Colluvial	3	22	75	14	2.68
Hume	Alluvial	0	19	81	51	2.71
Jindabyne	Residual	0	66	34	15	2.68
Lyell	Residual	1	70	29	13	2.61
Matahina	Residual	7	43	50	25	2.67
Pukaki	Glacial	10	48	42	13	2.70
Shellharbour	Residual	1	11	88	77	2.75
Waranga	Alluvial	0	21	79	54	2.69

TABLE II.
GEOTECHNICAL PROPERTIES OF SOIL SAMPLES

Soil		Test Name	Optimum Water Content (%)	Test Water Content (%)	Optimum Porosity	Test Porosity
Bradys	high plasticity sandy clay	BDHET001	35.0	35.8	0.52	0.52
		BDHET002	35.0	35.9	0.52	0.52
Fattorini	medium plasticity sandy clay	FTHET010	18.5	15.6	0.37	0.37
Hume	low plasticity sandy clay	HDHET001	21.0	21.4	0.39	0.40
		HDHET005	21.0	17.9	0.39	0.40
		HDHET006	21.0	22.6	0.39	0.40
		HDHET007	21.0	22.4	0.39	0.40
		HDHET009	21.0	22.7	0.39	0.40
Jindabyne	clayey sand	JDHET001	16.0	15.7	0.35	0.35
		JDHET005	16.0	13.8	0.35	0.35
		JDHET013	16.0	16.2	0.35	0.35
		JDHET016	16.0	18.3	0.35	0.35
Lyell	silty sand	LDHET014	10.0	8	0.25	0.25
Matahina	low plasticity clay	MDHET006	16.5	14.3	0.32	0.32
Pukaki	silty sand	PDHET003	8.5	8.6	0.20	0.20
Shellharbour	high plasticity clay	SHHET005	41.0	38.7	0.55	0.55
		SHHET009	41.0	37.9	0.55	0.55

no further manipulations are required to bring the model into line with the experimental data.

V. CONCLUSION

Many laboratory tests are commonly used to study internal erosion in a soil. One of them, the hole erosion test appears to be an efficient and simple means of quantifying the rate of piping erosion, but few attempts have been made so far to model this process. In the present modelling study, we started with the field equations for diphasic flow with diffusion and the equations of jump with erosion. After many simplifying assumptions, using asymptotic developments and dimensional analysis, some characteristic numbers were obtained, the two most significant of which are the kinetics of dimensionless number erosion and the erosion time.

A particular case was defined, involving low erosion kinetics. This situation arises when the erosion kinetics aremuch smaller than one. In this case, the influence of both the concentration and inertial effects can be neglected. An analytical scaling law was obtained for interpreting the hole erosion test with a constant pressure drop. Comparisons were made between the results of the present modelling study and previously published experimental data obtained in seventeen tests using nine different soils. These comparisons confirm the validity of our scaling law, which can therefore be used to interpret the results of hole erosion tests.

Further research is now required to determine whether this characteristic time could be used in practical situations to predict the development of internal erosion in hydraulic works.

ACKNOWLEDGMENT

The authors wish to thank Pr. Robin Fell and Dr. Chi Fai Wan for their valuable experimental data.

REFERENCES

[1] O. Brivois, *Contribution to strong slope erosion by a two-phase turbulent flow*, PhD, University of Aix-Marseille II, 2005.

[2] H. Chanson, *The Hydraulics of Open Channel Flows: An Introduction*, Butterworth-Heinemann, Oxford, UK, 1999.

[3] R. Fell and C.F. Wan , *Investigation of internal erosion and piping of soils in embankment dams by the slot erosion test and the hole erosion test* UNICIV Report No R-412, The University of New South Wales Sydney ISSN 0077 880X, 2002.

[4] M. A. Foster and R. Fell, Assessing embankment dam filters that do not satisfy design criteria. *Journal of Geotechnical and Geoenvironmental Engineering*, 127(5), 398–407, 2001.

[5] J.-J. Fry , *Internal Erosion: Typology, Detection, Repair*, Barrages and Reservoirs No. 6. French Comitee of Large Dams, Le Bourget-du-lac Cedex, 1997.

[6] P. Germain, Q.S. Nguyen and P. Suquet, Continuum Thermodynamics, *Journal of Applied Mechanics*, 50, 1010-1020, 1983.

[7] P.-Y. Julien, *Erosion and Sedimentation*, Cambridge University Press, 1995.

[8] P.-Y. Lagrée and S. Lorthois, The RNS/Prandtl equations and their link with other asymptotic descriptions. Application to the computation of the maximum value of the Wall Shear Stress in a pipe, *International Journal of Engineering Science* , 43(3), 352-378, 2005.

[9] L. W. Morland and S. Sellers, Multiphase mixtures and singular surfaces, *International Journal of Non-Linear Mechanics*, 36, 131-146, 2001.

[10] R.I. Nigmatulin, *Dynamics of multiphase media*, Book News, Inc. Portland, 1990.

[11] H. Schlichting, *Boundary layer theory* , 7th ed Mc Graw Hill, New York, 1987.

[12] C.F. Wan and R. Fell, Investigation of rate of erosion of soils in embankment dams, *Journal of Geotechnical and Geoenvironmental Engineering*, 30(4), 373-380, 2004.

[13] C.F. Wan and R. Fell, Laboratory Tests on the Rate of Piping Erosion of Soils in Embankment Dams, *Journal of Geotechnical Testing Journal,* 27(3), 2004.

TABLE III.
PARAMETERS OF THE HOLE EROSION TEST

Test	P_{fl} (Pa)	V_{fl} (m/s)	t_{fl} (10^{-3} s)	f_b (10^{-2})	R_e	$\tilde{a}_\phi$
BDHET001	79.96	2.20	1.36	1.65	6610	2.84
BDHET002	53.22	1.87	1.61	1.52	5606	3.07
FTHET010	93.78	2.57	1.17	1.42	7721	3.61
HDHET001	92.87	2.43	1.23	1.57	7298	3.30
HDHET005	66.13	2.22	1.35	1.34	6663	3.75
HDHET006	79.30	2.29	1.31	1.51	6875	3.46
HDHET007	79.43	2.33	1.29	1.47	6981	3.56
HDHET009	79.57	2.15	1.39	1.72	6452	3.04
JDHET001	77.74	2.26	1.33	1.53	6769	3.47
JDHET005	9.65	0.71	4.25	1.94	2115	2.68
JDHET013	53.22	1.52	1.98	2.32	4548	2.29
JDHET016	6.91	0.63	4.73	1.72	1904	3.15
LDHET014	7.96	0.81	3.70	1.21	2433	4.57
MDHET006	129.00	2.93	1.03	1.51	8779	3.57
PDHET003	16.43	1.02	2.93	1.57	3067	3.87
SHHET005	106.30	2.68	1.12	1.48	8038	3.05
SHHET009	102.39	2.71	1.11	1.39	8144	3.23
WBHET001	105.91	2.71	1.11	1.44	8144	3.58

TABLE IV.
RESULTS OBTAINED WITH THE SCALING LAW

Test	τ_c (Pa)	V_{er} (10^{-5} m/s)	t_{er} (s)	c_{ref} (10^{-5})	k_{er} (10^{-4} s/m)	$k_{er}V_{fl}$ (10^{-4})
BDHET001	76.07	1.35	223	11	3.02	6.65
BDHET002	50.93	1.43	210	14	4.80	8.97
FTHET010	6.63	4.10	73	39	8.57	22.05
HDHET001	92.87	0.94	319	9	2.01	4.88
HDHET005	66.13	1.00	299	10	2.93	6.50
HDHET006	76.00	0.18	1712	2	0.44	1.01
HDHET007	79.41	0.50	600	5	1.26	2.93
HDHET009	74.42	0.14	2183	1	0.35	0.75
JDHET001	72.32	2.26	133	25	5.89	13.30
JDHET005	6.92	0.46	647	16	9.59	6.76
JDHET013	49.66	0.79	380	13	3.03	4.59
JDHET016	6.42	0.26	1165	10	7.73	4.90
LDHET014	7.95	5.22	57	185	139.19	112.86
MDHET006	128.22	0.71	424	6	1.13	3.31
PDHET003	13.85	0.71	424	21	10.05	10.28
SHHET005	106.20	1.98	152	13	3.22	8.63
SHHET009	99.77	0.31	975	2	0.52	1.40
WBHET001	105.81	1.41	213	12	2.62	7.12

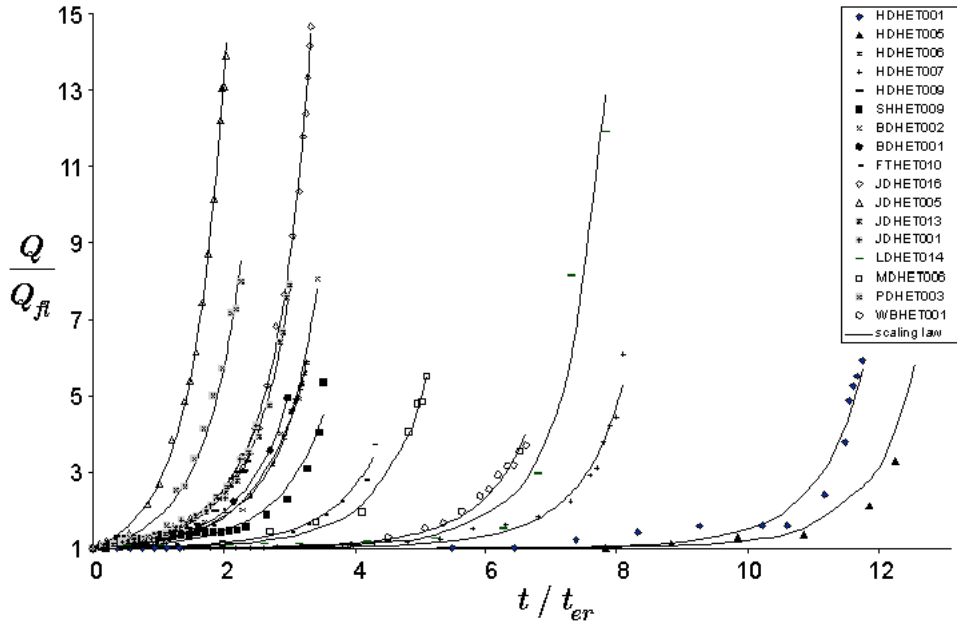

Figure 2. Hole Erosion Test, test(symbols) versus model(continuous lines). Dimensionless flow is shown as a function of dimensionless time. The experimental data were based on [2].

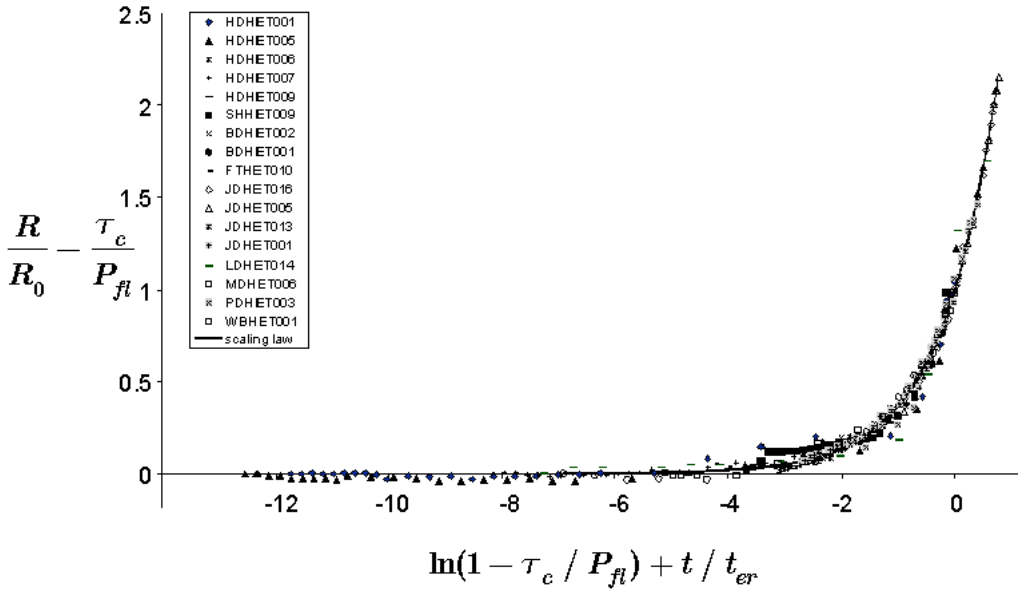

Figure 3. Hole Erosion Test, test(symbols) versus model(continuous lines). Dimensionless radius is shown as a function of dimensionless time. The experimental data were based on [2].